Nano Energy 60 (2019) 440–448

Contents lists available at ScienceDirect

Nano Energy

journal homepage: www.elsevier.com/locate/nanoen

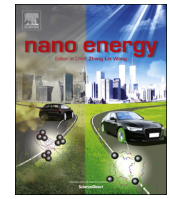

Full paper

Intuitive-augmented human-machine multidimensional nano-manipulation terminal using triboelectric stretchable strip sensors based on minimalist design

Tao Chen[a,b,c,1], Qiongfeng Shi[b,c,d,1], Minglu Zhu[b,c,d,e], Tianyiyi He[b,c,d,e], Zhan Yang[a,*], Huicong Liu[a,*], Lining Sun[a], Lei Yang[f], Chengkuo Lee[b,c,d,e,*]

[a] Jiangsu Provincial Key Laboratory of Advanced Robotics, School of Mechanical and Electric Engineering & Collaborative Innovation Center of Suzhou Nano Science and Technology, Soochow University, Suzhou, 215123, P.R. China
[b] Department of Electrical and Computer Engineering, National University of Singapore, 4 Engineering Drive 3, Singapore 117576
[c] Center for Intelligent Sensors and MEMS, National University of Singapore, E6 #05-11F, 5 Engineering Drive 1, Singapore 117608
[d] Hybrid-Integrated Flexible (Stretchable) Electronic Systems Program, National University of Singapore, E6 #05-4, 5 Engineering Drive 1, Singapore 117608
[e] NUS Suzhou Research Institute (NUSRI), Suzhou Industrial Park, Suzhou, 215123, China
[f] Orthopaedic Institute and Department of Orthopaedics, Soochow University, Suzhou, 215006, P.R. China

ARTICLE INFO

Keywords:
Triboelectric Effect
Nanomanipulation
Stretchable
Control terminal

ABSTRACT

Sensors based on triboelectric nanogenerators have been widely used for energy harvesting and sensing applications, however, the applications of multidimensional information perception and interactive control are insufficient. In this paper, we present an ultra-stretchable triboelectric strip sensor (TSS) using triboelectric mechanism for controlling the objects in three-dimensional space. This facile and low-cost TSS is mainly composed of a parallel structure including three symmetric sensor strips fixed on the base and a mobile stage connected with them. Based on the coupling effect of triboelectrification and electrostatic induction, the length changes of each strip with the same finger contacting point generate different signal output ratios from two terminal electrodes, functioning as the interactive interface for multi-dimensional sensing and controlling. Hence, the parallel sensor strips structure can realize the sensing and controlling in three degrees of freedom of linear motion and two degrees of freedom of rotational motion, and resultant sensing ranges are X, Y, Z, α and β (20 mm, 20 mm, 30 mm, 36°, and 36°). In terms of manipulation, this is simpler than the conventional controller with rigid structure and includes additional space dimensions. Furthermore, demonstration of the TSS as human-nanomachine terminal to control the nanomanipulator in scanning electron microscope (SEM) is successfully realized with the accuracy of 10 nm. The proposed TSS shows great potential for the applications in automated control, robotics control, and Internet of Things (IoT).

1. Introduction

Development of sensors and actuators technology provides a technical basis for precision humanoid operation [1–3]. The properties of smaller structures and materials, such as nanotubes, graphene *etc.*, have been characterized to explore their applications in nanophotonics, medicine, nanoelectronics and biology [4,5]. The successful assembly, operation and investigation of carbon nanotubes (CNT) or graphene in scanning electron microscope (SEM) environment provide a solution to the above research fields [6,7]. Furthermore, there are inaccessible, unforeseeable dangerous or unavoidable challenges for human to interact or perform complex tasks in environments such as equipment maintained in vacuum, undersea, space and nanometer scale, *etc.* For effective interactions between humans and intelligent or automated systems, a variety of control terminals with different working mechanisms are researched such as touch screen, keyboard or rocker structure [1,3]. But in most cases, these control mechanisms are indirect controls that need complex instruction analysis and calculation to correspond to the movement state of the object to be manipulated. The direct correspondence and real-time reappearing of the control terminal and the object manipulated in the movement posture is an important research aspect for the human-computer interaction. Therefore, how to

* Corresponding authors. Department of Electrical and Computer Engineering, National University of Singapore, 4 Engineering Drive 3, 117576, Singapore.
E-mail addresses: yangzhan@suda.edu.cn (Z. Yang), hcliu078@suda.edu.cn (H. Liu), elelc@nus.edu.sg (C. Lee).
[1] These authors contributed equally to this work.

https://doi.org/10.1016/j.nanoen.2019.03.071
Received 21 January 2019; Received in revised form 3 March 2019; Accepted 21 March 2019
Available online 26 March 2019

optimize the interaction process and improve operational performance are the focus of the study. So far, the most intuitive way is to directly convert the control operation from human into the process of object motion through the control terminal. Recently, many different types of sensors are applied to detect the physical activities, intentions, and emotions of humans [8–12]. To realize motion control by human intention, the precise measurement and analysis of sensors are the most critical and basic requirements [13–15]. Nowadays, there has been a hot issue in development research of stretchable and flexible material because it has potential applications as tactile, pressure, and motion sensors [16–22]. Typically, in order to meet the requirements of motion control devices, the motion sensors must be equipped with an internal power supply. At present, a great deal of self-powered sensors based on triboelectric nanogenerators (TENGs) have been extensively studied and reported [23–29]. Self-powered tactile sensors based on TENGs have the potential applications to detect pressure change without an external power source [30–35]. In addition, the self-powered systems can avoid the complex electric circuits [36–41].

Among various triboelectric based self-powered sensors, pressure and tactile sensing are important research areas in motion detection [42–45]. Self-powered sensors based on TENGs have many advantages, such as the flexible nature, self-powered functionality and simple structure [46–49]. Comparing the stretchable and flexible devices based on TENGs compared to their rigid counterparts, the premise of integration with the moving parts of machinery is mechanical compliance [50–52]. In addition, the flexible TENGs as the power sources and multifunctional sensors for human motion have been designed to meet the development of the deformable and stretchable electronics [53–57]. P. K. Yang et al. used paper to design origami TENGs. It shows a light weight, a high degree of flexibility, and so on [53]. In the same year, they assembled a wavy-structured Kapton film and serpentine-patterned electrodes to fabricate a flexible TENG [54]. J. Chun et al. combined a highly-stretchable piezoelectric hemisphere and thin film TENG sensor for motion detection of human body [56]. J. Bian et al. presented an excellent uniaxial stretchable sensor to detect the ambient mechanical energy [57]. Besides, the stretchable materials and electrodes are essential part to connect the working circuits and the flexible TENG [58,59]. B. U. Hwang et al. presented a sensor composed of multifunctional nanocomposite materials to detect the motion of the human body. The sensor is stretchable, self-powered and patchable [60]. In the application to hand joints, G. H. Lim et al. proposed TENG sensor with a durable and stretchable nanosheet [61].

The detection of three and more degrees of freedom (DOFs) for a human-machine interface is the research trend, especially, it requires complex design and complicated control system to realize the teleoperation. Moreover, in order to achieve more degrees of freedom, it is necessary to increase the hardware structures and control difficulty [62–64]. In previous works, a simplified tactile sensor configuration reported by Wang's group and Zhang's group has been developed as the 2D sensing and controlling interface. When a fingertip touches the surface of this sort of 2D flexible tactile sensor, the ratio of the output voltage from the two pairs of electrodes is used to derive the fingertip position [65–68]. With the aid of flexible grid pattern on tactile sensor surface, T. Chen et al. has further enabled this flexible 2D tactile sensor to read the trajectory drawn by fingertip. Furthermore, z-axis position information created by fingertip contacting a stretchable flexible strip is again determined by the ratio of output voltage from electrodes at the two ends of the strip. Such z-axis position information is added on the 2D trajectory information to help robotic manipulator successfully writing 3D patterns at the scale of human living environment [69].

In this paper, we present an ultra-stretchable triboelectric strip sensor (TSS) for controlling the attitudes of the object in space. This low-cost, facile-designed device mainly consists of a parallel structure including three symmetric strips. Each of the strips is used as a spatial sensor, and a single strip can achieve a longitudinal sensing resolution of 3 mm. Based on the coupling effect of triboelectrification and electrostatic induction, the length changes of each strip in this parallel mechanism generates different signal output ratios as the interactive interface when the fingertips knock for auto controlling and multi-dimensional information sensing. The entire parallel sensor structure can realize five DOFs control: three DOFs of linear motion, *i.e.*, X, Y, Z (20 mm, 20 mm, 30 mm) and two DOFs of rotational motion, *i.e.*, α, β (36°, 36°). The intuitive five-dimensional positioning projection in space can be achieved using the TSS, which is simpler than the traditional rigid structure and adds the space dimensions. Meanwhile, the detection mechanism using the voltage ratio method avoids the influence of environmental humidity and uneven force. Demonstration of the TSS device as the teleoperation terminal for multidimensional control in SEM is successfully realized. The proposed TSS shows the great potential of robotic control applications, automated control and IoT.

2. Results and discussion

2.1. Design and structure of the TSS device

The teleoperation system allows operators to control remote targets through master-slave devices. It is mainly used in military, industrial, medical, and some human inaccessible or dangerous environments to perform complex tasks as shown in Fig. 1a. In this paper, the TSS device is designed as a teleoperation control terminal aiming to the nanomanipulator control in SEM as shown in Fig. 1b. The symmetric TSS device is composed of a basement, a mobile stage, and three strips with three pairs of electrodes located at both ends of each strip as shown in Fig. 1c. The mobile stage is connected with the basement through the three strips. During the stretching of the strip, fingertip tapping on the fixed point of the strip will result in varying voltage ratios corresponding to the different lengths, due to the changes of distances from the contact point to two opposite terminal electrodes. The structure diagram of the strip with two opposite electrodes is demonstrated in Fig. 1d. The working mechanism of the triboelectric strip sensor is shown in Fig. 1e. By detecting the length variation of three strips, the space motion state of the mobile stage can be derived synthetically. Thus, the multi-dimensional motion control operation is carried out through the motion attitude of the mobile stage. For initializing the device during assembling, all three strips are pre-stretched by 10 mm when connecting the inner mobile stage with the outer basement. In this way, each strip can perform both stretching and contraction motions without over loose, so as to realize the motion detection of the mobile stage for all directions. The length detection method and the experiment will be elaborated in detail in the next section. The strip consists of silicone rubber as the main structure and two opposite electrodes fabricated with starch-based hydrogel PDMS elastomer (HPE). HPE has good electrical and stretchable properties, which can greatly match the stretching needs of this device.

Each movement detection of the platform requires the three fingers knocking on the corresponding strips to determine the spatial position of mobile stage at this moment. A pair of opposite electric fields between two layers with different electron affinities is induced when the finger touches the silicone rubber surface and retained within this contact area. As the finger is separated away, the potential differences are created that need to be balanced. For each silicone rubber strip, according to the distance differences between finger and two counter electrodes, each electrode will obtain different amount of charges after releasing of finger and lead to different currents and voltages which can be measured. The induced charges are repelled back to ground after the finger contact the silicone rubber strip again and result negative current flows. Therefore, the touching positions can be identified through the variations of the current and voltages between two counter electrodes.

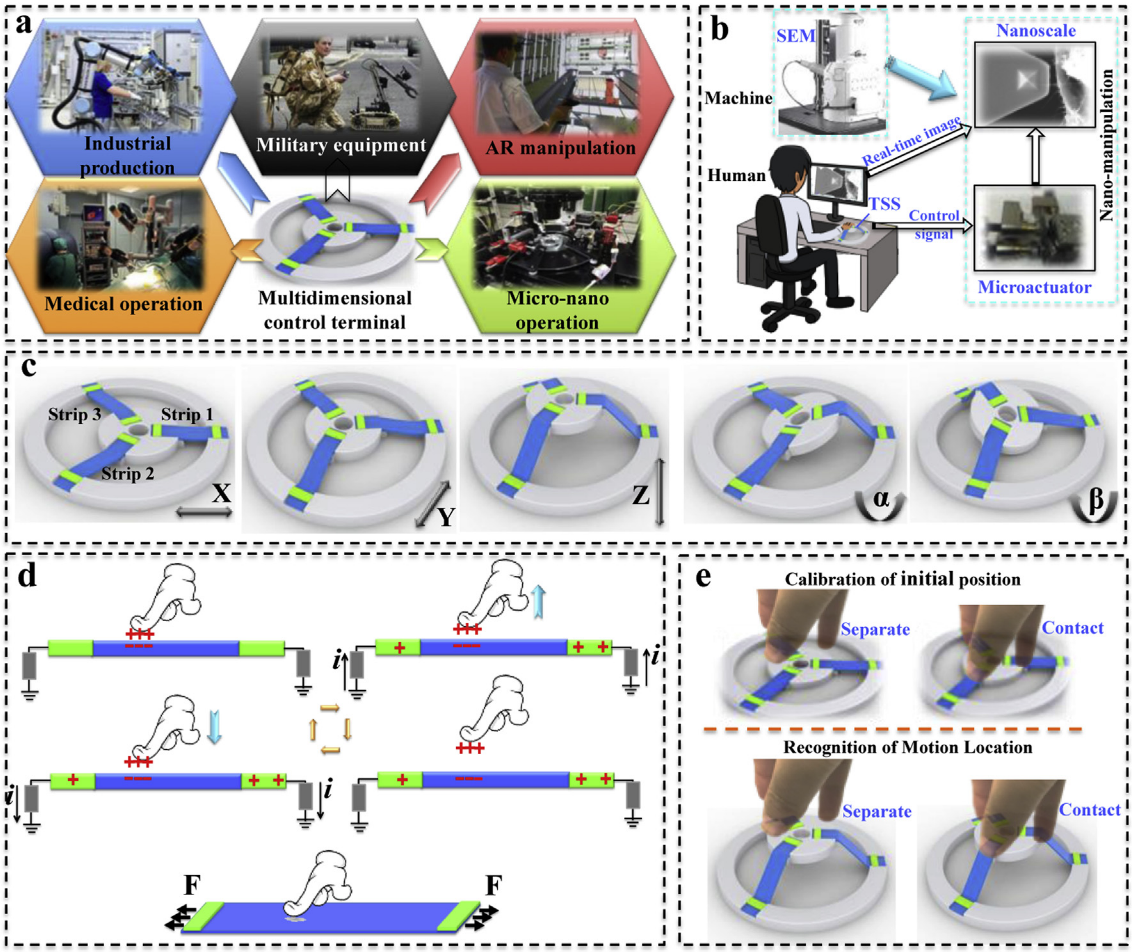

Fig. 1. Application areas, conceptual illustration and working principle of the TSS device. **A** Multidimentional control terminal can be widely used in many fields, such as military, medical treatment, *etc*. **B** The diagram of human-machine nano-manipulator control in SEM. **C** The five attitude diagrams of the TSS device. They are three-dimensional linear motion of X, Y, Z and two-dimensional rotational motion of α, β, respectively. **D** Schematic diagram of the strip and the electrostatic analysis of the contact process. **E** Operation sketch of the TSS device in man-machine interaction process.

2.2. Working mechanism and structure of the stretchable electrodes

By using analogue analysis to characterize the location identification of the strips [68–70], the output voltages against the counter electrodes are studied accordingly to investigate the relationship. The corresponding electric fields at each electrode for finger touching are represented in Equations S1-S3 (Supporting Information). When h is zero, $V_{E1} = V_{E2} = 0$ as the electric field is maintained between two contacted surfaces (finger/silicone rubber). The voltage of two electrodes can be defined as $V_{E1} = -kQ/x$ and $V_{E2} = -kQ/(l-x)$, along with the increasing of the height h. It indicates that the separation distance of finger away from silicone rubber can alter the output voltages of two electrodes. Therefore, according to the characteristics of triboelectrification, it is assumed that the fingertip raised a high distance, and then the V_{E2}/V_{E1} is similar to the ratio of $x/(l-x)$. The simulation results of V_{E2}/V_{E1} of the strip with counter electrodes during the changing of contact locations are illustrated in Figure S2. Based on the great monotonicity, the location identification of finger touching can be proved as feasible and reliable.

The conventional metallic based electrode is disadvantageous for motion sensing applications, obstructing the sensors or devices to tolerate mechanical deformations in practical uses. In order to achieve better structural stretchability, flexibility and simple design, the electrodes of TSS are fabricated by HPE in this design. As the operation principle is shown in Fig. 2a, HPE is inserted and fixed inside the silicone rubber strip. The contact electrification happens during the contact between finger and silicone rubber. The variations of external electric fields can be revealed through HPE due to its conductivity. For a typical finger tapping motion, the short circuit current and open circuit voltage of HPE-silicone rubber are shown in Fig. 2b. The photos of the as-fabricated TSS device are illustrated in Fig. 2c and d. Because the strips are stretchable and flexible, in order to ensure the range of motion and accuracy of detection, the strips are assembled in the device with a 10 mm pre-tension length and the maximum stretch of each strip is set as 20 mm. To limit the movement of the mobile stage, height limit and area limit are added on the basement. Dimensions of the TSS are listed in Table S1 (Supporting Information). The TSS device is designed as a one-handed operating mode. The middle finger is used to operate the stage for multi-dimensional movement, and the thumb, index finger and ring finger are responsible for tapping three strips. The corresponding structure is added in the stage to facilitate one-handed operation as shown in Fig. 2e and f.

The electrical performance of HPE is characterized through controlled stretching by the linear motor, the results under 1.5 V voltage are shown in Figure S3 (Supporting Information). According to the tested data, the HPE electrode material is capable of sustaining a good electrical conductivity within a 200% strain. The HPE is used as the electrodes combined with silicone rubber to fabricate the strip sensors.

2.3. Working mechanism of the strip

Based on the analog positioning method, a stretchable strip is

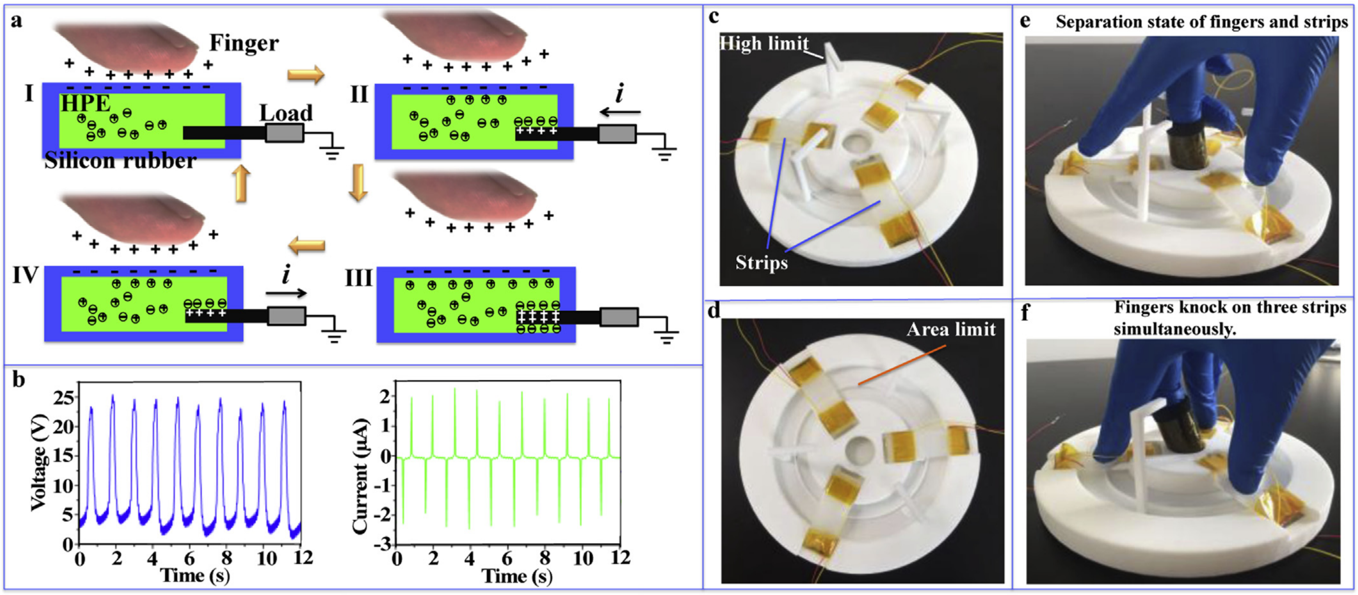

Fig. 2. The TENG based working mechanisms of the HPE electrode, and the electrical characteristics of the electrode. **A** Schematic illustration of TENG based working principles of the HPE electrode in single electrode mode. I: contact state; II: separating state; III: separated state; IV: approaching stage. **B** Open-circuit voltage and short-circuit current of TSS based on the HPE electrode. **C** and **D** Photographs of the TSS device. In order to limit the movement of mobile stage, high limit and area limit are added on the structure of the basement. **E** The middle finger is used to operate the stage for multi-dimensional movement. The thumb, index finger and ring finger are responsible for tapping three strips. Three fingers are separated from the strips when the stage is moving. **F** Three fingers tap the strips when we need to detect the location at a certain time. On the stage, three inclined planes are designed under the strips to determine the focus of finger tapping.

proposed as the spatial sensor. One end of E1 electrode of the strip is fixed, the electrode E2 is movable under tensile stress with respect to E1 (as shown in Fig. 3a). The output voltage ratio of the two electrodes (V_{E2}/V_{E1}) is obtained during the contact and separation of finger and silicone rubber with a constant distance from E1. Furthermore, the strip is stretched by a certain length, the decrement of voltage ratio is determined as we re-touch the same position (reference point) at a constant distance with respect to the E1 electrode. The further decreasing of the ratio is observed when the stretching length increases continuously. Hence, by utilizing this mechanism, the extended length of the E2 side can be measured through touching the reference point which is fixed from E1. In other word, the displacement of strip under stretching, the stretching velocity and acceleration of the E2 electrode can be measured with a constant contact frequency. As shown in Fig. 3a, the stretching capability is demonstrated under various operation scenarios. The theoretical analysis shows that the measuring principle of the strip sensor is independent of the intensity of the knocking force. As a verification, different forces are applied to knock the same point. The ratio of the two electrodes is equal within the error range as shown in Fig. 3b. Therefore, the knocking force does not affect the calculation of the length and position of the strip sensor. To show the reliability of the strip design, 10,000 repeated stretch tests are carried out through a linear motor. During the testing process, the strip and the supporting plane are constantly rubbing, which can effectively simulate the knocking effect. Before and after the test, the finger knocks the strip reciprocally between the two electrodes, recording the corresponding signal characteristic curves as shown in Figure S4a and b. The stable voltage curve can be maintained after 10,000 stretch cycles, showing that these strips are proved to be valuable in the reliable design.

To select suitable strip size for the TSS device, the size variations of strips are analyzed based on the output voltage ratio. The trends of ratio change from the output voltages of two counter electrodes is shown in Fig. 3c as the elongation changes. It is clear that the same elongation gives similar voltage ratio, indicating that the geometry of the strip does not have significant influences on the output amplitude during stretching. Such characteristics provide an important prerequisite for making displacement sensors. Firstly, the resolution of stretch displacement is characterized by detecting the displacement and velocity parameters. Corresponding to different initial length, Fig. 3d shows the relationships of the stretch displacement with the error bars of V_{E2}/V_{E1}. The resolution decreases gradually with the increase of stretching length. And the resolution decreases gradually with the increase of initial length. Therefore, we chose the strips with an initial length of 3 cm to achieve higher resolution. As shown in Fig. 3e, it can be seen that at every 3 mm of stretching length, the ratio of voltage value can be distinguished without overlapping area at each measuring point. Therefore, the resolution detection of strip stretching has achieved a resolution of 3 mm within the scope of 20 mm. The curves of the voltage ratios with time under the stretch velocity of 3 mm/s, 4 mm/s and 5 mm/s are shown in Fig. 3f. Movie S1 (Supporting Information) shows the curves of the two electrode voltages during the stretching process.

Supplementary video related to this article can be found at https://doi.org/10.1016/j.nanoen.2019.03.071

2.4. Analysis and test of TSS device as the control terminal

The strips are assembled in the device with 10 mm pre-stretched length and the maximum stretch length of each strip is set as 20 mm. In this way, the control precision of the device can be guaranteed and the motion space is appropriate. The motion range of TSS device is analyzed as shown in Figure S5. Considering the pre-stretching length of 10 mm sensor and the motion accuracy, the motion range of the device in the plane is expressed by the overlapping area of stretching and contracting of the sensor, as shown in Figure S5 (Supporting Information) under the above restricted condition. According to the cosine theorem, the relationship of the mobile stage attitudes and the lengths of the strips are calculated and illustrated in Figure S6 (Supporting Information). As the maximum stretching limit of the strip, the Z-direction displacement of the device is calculated to be 30 mm by the size of strip 1, as shown in Figure S6c. At the same time, the height limiting stopper is designed to limit the moving range of the mobile stage in the Z direction. Similarly, based on the length limit of the strips and the size of the mobile stage, the maximum tilting angle of the stage is calculated

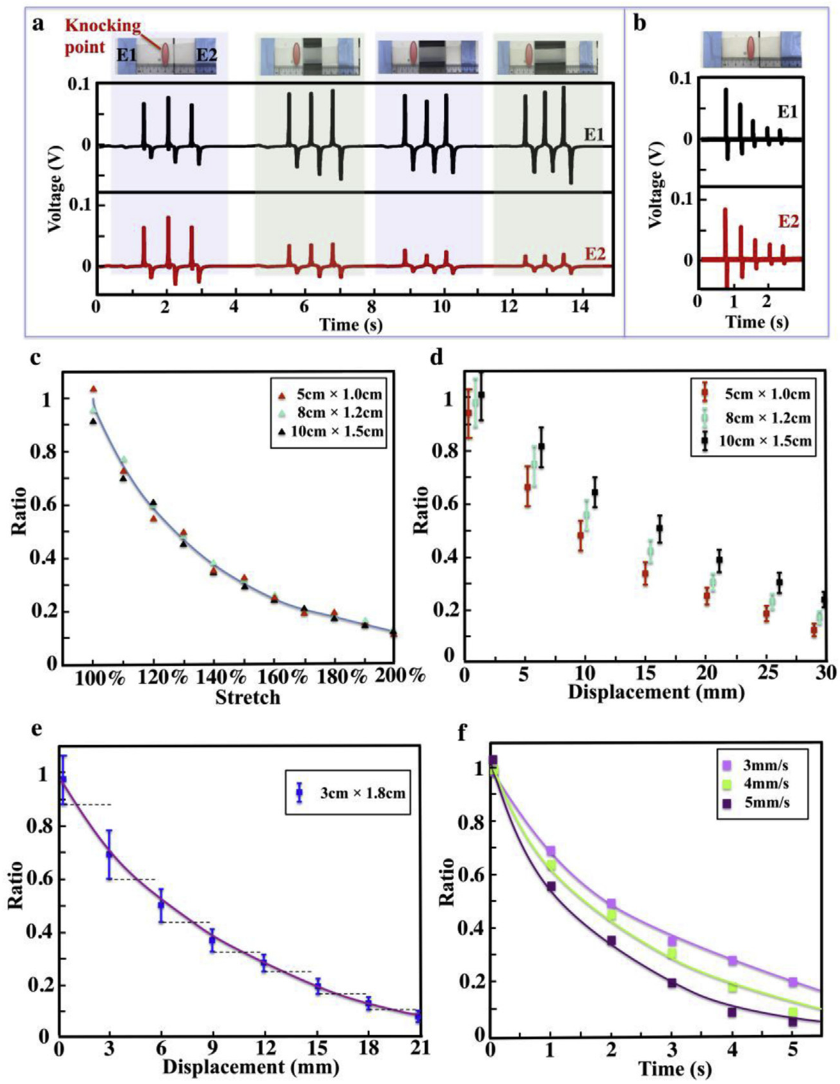

Fig. 3. Electrical measurements of the finger knocking on the silicone rubber layer, and the analysis of the stretching process. **A** The voltage waveform of the two electrode voltages with the increase of the stretch length. **B** Knocking the same point using different force, the ratio of the two electrodes is equal in the error range. Therefore, the knocking force does not affect the calculation of length and position. **C** The ratio change trend of two electrodes voltages with the change of the stretch percentage. **D** Relationship of the error bars of V_{E2}/V_{E1} with the stretch displacement corresponding to different initial length. **E** The error bars of E2/E1 with the stretch displacement corresponding to initial length 3 cm of strip. **F** Detected ratio of V_{E2}/V_{E1} on the strip over time. The stretchable displacement with time can be derived. The corresponding stretching velocities are 3 mm/s, 4 mm/s, and 5 mm/s respectively.

to be about 36°, as shown in Figure S6d and e.

In order to verify the theoretical calculation, we measured the displacements and angles of the mobile stage with five DOFs, as shown in Fig. 4. A number of points are selected for testing in full range of each DOF and marked in the figures. The theoretical curves in Fig. 4 are derived from Figure S5 (Supporting Information). The voltage output curves of the stage in the X, Y, Z, α and β directions are given respectively. The motion of mobile stage is repeated for more than 3 cycles. In order to elevate the accuracy and reliability of measurements, the peak-peak output voltages are calculated. The results show that the measured points in the selected position are distributed along the theoretical curve, which proves that the design can realize the attitude control of five DOFs.

According to the structural design of the device, the motion in multiple directions can be realized in the XY plane, and the angle can be calculated by the length relation of three strips. Firstly, the length variations of the three strips are calculated theoretically, when the stage moves along the area limit boundary from 0 to 180°, as shown in Figure S7a and b. The analysis from the previous section shows that the length resolution of the strip is 3 mm. In terms of the maximum slope of the curve for each strip in Figure S6b, the angle changes at least about 22°–25° when the length of the strip changes more than 3 mm. In order to detect the resolution of the angle, we measure 50 times for every 30° and record the signals. The length of each strip is calculated by the ratio relation of the signals. Then, the corresponding motion angle of the mobile stage is derived by the lengths of three strips. The angle deviated from the measurement direction is drawn from the calculated angle values, as shown in Figure S7c. It can be seen that at every 30°, the deviation areas can be clearly distinguished without data overlapping at each measuring point. In addition, 180°–360° and 0–180° are symmetrical structures in this device. Therefore, we defined that the angle detection in XY plane having a resolution of 30° within the scope 360°.

2.5. Applications in the micro-nano manipulation

As the motion sensor in the control application plays a fundamental role in the auto-control, virtual reality (VR) or IoT, the precise capture and recognition of motion behavior, especially the multi-dimensional inversion process, is the key for facilitating those applications. The motion perception of the TSS mobile stage is achieved directly by the spatial sensing of the three strips. In order to show the practicability, the TSS device is fabricated by 3D printing and controlled by hand as shown in Fig. 2e and f. A real-time monitoring of hand behavior to control the manipulator in SEM is demonstrated in Fig. 5. It is clearly seen that the output signals of the TSS have obvious distinctions on different attitudes and locations, with different control purpose. Fig. 5a shows the SEM device and the micro-nano positioning platform inside. The control terminal (Fig. 5b) is directly connected with A/D converter, which is connected to the controller through a serial port. The schematic diagram of the electrical connection and components used in the

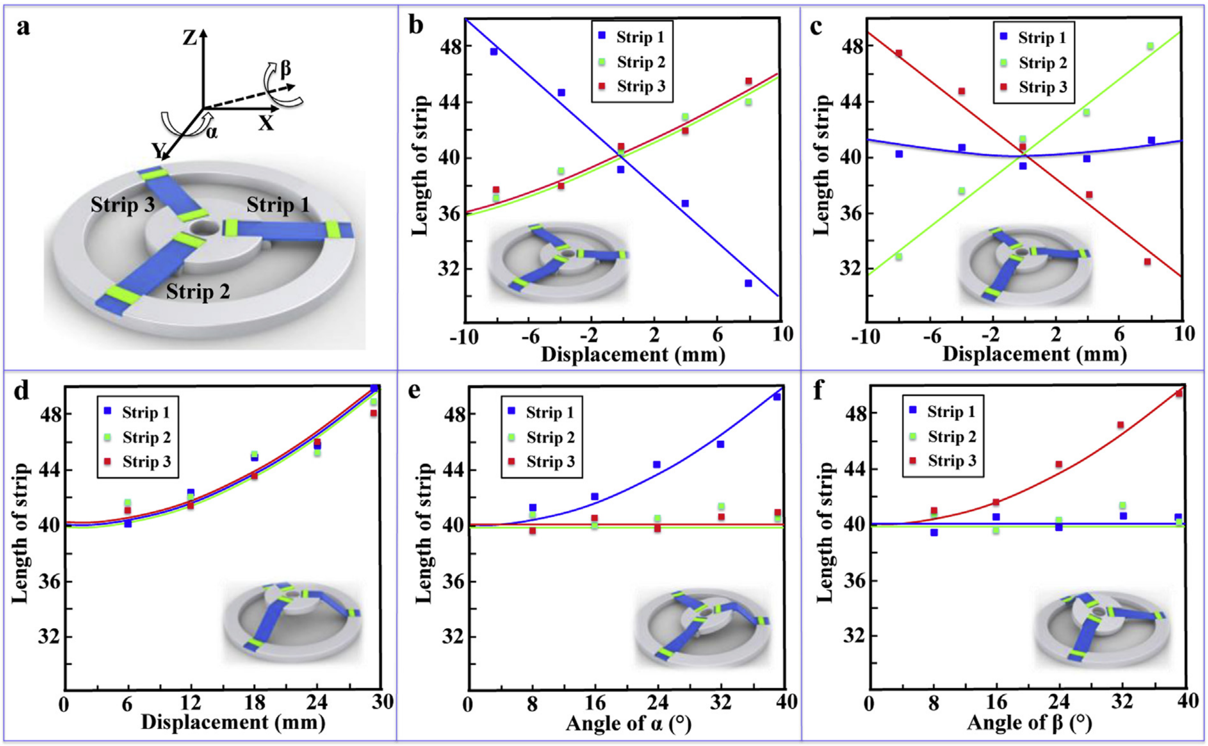

Fig. 4. The tests of displacements and angles of the mobile stage with five DOFs. The solid line in the graph is the theoretical calculation curve. **A** Diagrammatic sketch of the mobile stage. **B** X DOF of the stage. **C** Y DOF of the stage. **D** Z DOF of the stage. **E** α DOF of the stage. **F** β DOF of the stage.

demonstration is shown in Figure S8. Firstly, the data acquisition card collects the voltage values of three pairs of electrodes on the strips. After filtering and amplifying, the analog values are converted to digital signals. The voltage ratio of corresponding electrode is then analyzed by the computer program to obtain the length of strip. Hence, by calculating and analyzing the lengths of three strips, the attitude information of the mobile stage in five dimensions can be derived and become the motion parameters of the motor in SEM for the computer to send the command to drive each motor. The program can realize two operation modes: absolute coordinate mode and relative coordinate mode. In absolute coordinates mode, the origin is located at the initial point. The motion direction of the end of manipulator matches to that of the mobile stage center, but with the reduced proportion in terms of displacement distance. The relative coordinate mode can realize specific direction and movement distance, without setting initial point, and can realize multi-direction and long-distance operation. In the coordinate system, the long-distance motion of the manipulator can be realized by multiple tapping to repeat the same motions further, which is not affected by the motion range stopper of the mobile stage. And hence, by controlling the motion length along two axes individually, the end of manipulator can move to any point in practical operation. The schematic diagram of absolute coordinate and relative coordinate control method is shown in Figure S9. This method realizes the isolation between the control part of TSS device and the control circuit of the motors in SEM, effectively conveys the control command and ensures the motion accuracy of the platform in SEM.

The nanomanipulation device with four DOFs is designed to manipulate the nanometer-scale objects and construct nanodevices inside the SEM. The SEM was used to derive the real-time monitor for the manipulation of nanometer-scale objects. The manipulator device has four DOFs with three linear motions (X, Y, Z directions) and a rotation direction. The CNT is picked up by the surface adhesion force between the AFM probe and CNT. The visual feedback control is used to realize the multi-manipulators operating inside the SEM chamber. Fig. 5c and d are the photographs of the micro-nano positioning platform outside and inside SEM. Fig. 5f shows the output signals corresponding to the attitudes measured from five motion behaviors of X, Y, Z, α and β. Three specific positions of five DOFs are selected in the figure, which are the maximum, the minimum and the middle values of each DOF. The voltage results on each electrode of three strips are tested corresponding to these positions. Fig. 5g shows the moving schematic diagram of each DOF of the stage and each strip length calculated by the measured voltage values in the three specific positions of the stage. To highlight the ability of the TSS device and expand its applications, the demonstration of manipulating a CNT is shown in Fig. 5e and Supporting Movie 3, Movie 4 and Movie 5. By setting up the program, the demonstrations of Movie 3 and Movie 4 is adopted the absolute coordinate mode. The demonstration of Movie 5 is relative coordinate control mode, that is to say, under the same direction of command, the motor always moved in the same direction, which can realize the operation of large distance. Figure S10 shows the video captures of the demonstration of the manipulator in macro scale and operation of CNTs in micro scale. The micro-actuator in SEM can achieve motion accuracy less than 10 nm (to the motion accuracy of motors in SEM), so the CNT operation of nano-scale can be controlled by human-machine through the scale reduction of motion parameters in the program. This micro-nano manipulation result confirms the excellent performance of TSS device in the perceptual and control application of the robotics, VR and IoT based industry applications, *etc.*

Supplementary video related to this article can be found at doi:mmcdoino

3. Conclusion

In summary, a nano-manipulation control terminal using TSS is proposed, and the comprehensive theoretical modelling and experimental characterizations are investigated. This device made up of three sensor strips can detect five DOFs including three linear DOFs and two rotational DOFs in the space to realize 3D operation of the objects. Based on triboelectric working principle, the length changes of each

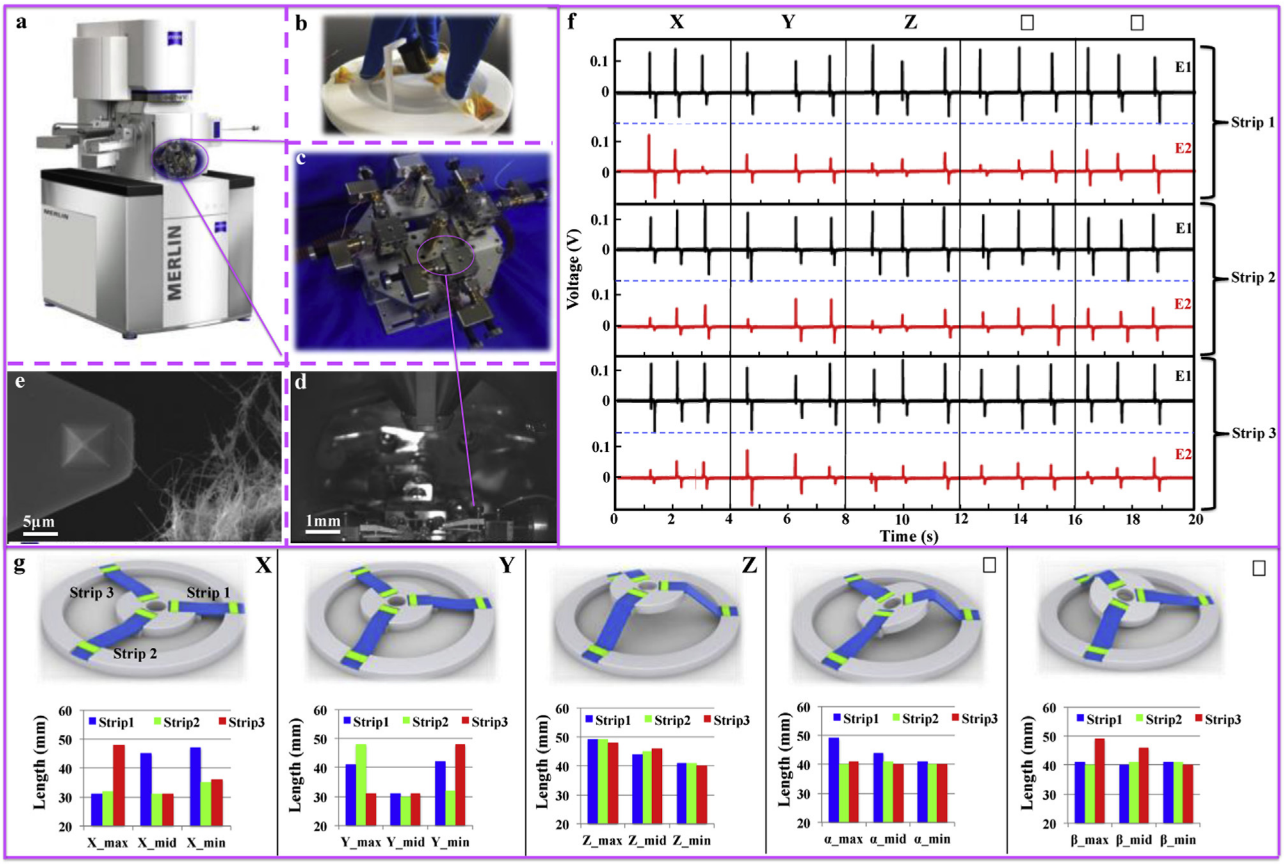

Fig. 5. The demonstration of the TSS device controlling the manipulator in SEM. **A** SEM with the manipulator inside. **B** The manipulator. **C** Photograph inside the SEM cavity. **D** Operation of carbon nanotube. **E** Multi-point manipulation of carbon nanotubes. **F** The voltage results on each electrode of three strips are tested when the stage is at the maximum, minimum and middle positions of five DOFs. **G** The moving schematic diagram of each DOF of the stage. Each strip length is calculated according to the measured voltage signal in the three specific positions of the stage. The output waveforms of each electrode corresponding to three strips are illustrated. Each of the five sets of data has three waveforms, which are the voltage output curves of the electrodes when the stage reaches the three specific locations.

strip can be derived through an analog ratio method. Analyzing the length relationships of three strips, the TSS device structure can realize the sensing and control of X, Y, Z, α, β (20 mm, 20 mm, 30 mm, 36°, 36°), respectively. In term of XY plane detection, it can resolve the direction with a step of at least 30°. Through the manipulation of the nano-positioning platform in SEM, the micro-nanoscale operation of CNT is realized with the accuracy of 10 nm. The intuitive five-dimensional positioning projection in space can be achieved using the TSS, which is simpler than the conventional controller with rigid structure and includes additional spatial dimensions. This nano-manipulation control terminal shows great potential with the minimalist design and very low-cost materials for the applications in remote robotics control, automated control and Internet of Things (IoT) based industry applications, *etc.*

Acknowledgement

This research was funded by The National Natural Science Foundation of China grant (No.61673287, 61773275, 51875377); National Key Research and Development Program of China (2018YFB1107602); Qing Lan Project; HIFES Seed Funding-2017-01 grant (R-263-501-012-133) "Hybrid Integration of Flexible Power Source and Pressure Sensors" at the National University of Singapore; Agency for Science, Technology and Research (A*STAR), Singapore and Narodowe Centrum Badań i Rozwoju (NCBR), Poland Joint Grant (R-263-000-C91-305) "Chip-Scale MEMS Micro-Spectrometer for Monitoring Harsh Industrial Gases".

Appendix A. Supplementary data

Supplementary data related to this article can be found at https://doi.org/10.1016/j.nanoen.2019.03.071.

References

[1] B. Fang, F. Sun, H. Liu, D. Guo, W. Chen, G. Yao, Robotic teleoperation systems using a wearable multimodal fusion device, Int. J. Adv. Robot. Syst. 14 (2017) 1–11.
[2] Z. Fan, X. Tao, X. Fan, X. Li, L. Dong, Sliding probe methods for in situ nanorobotic characterization of individual nanostructures, IEEE T. Robot. 31 (2015) 12–18.
[3] Y. Gao, Z. Du, X. Gao, Y. Su, Y. Mu, L. Sun, W. Dong, Implementation of open-architecture kinematic controller for articulated robots under ROS, Ind. Robot 45 (2018) 244–254.
[4] Z. Fan, X. Tao, X. Fan, X. Zhang, L. Dong, Nanotube fountain pen: towards 3D manufacturing of metallic nanostructures, Carbon 86 (2015) 280–287.
[5] R. Garcia, A.W. Knoll, E. Riedo, Advanced scanning probe lithography, Nat. Nanotechnol. 9 (2014) 577–587.
[6] C. Shi, D.K. Luu, Q. Yang, J. Liu, J. Chen, C. Ru, S. Xie, J. Luo, J. Ge, Y. Sun, Recent advances in nanorobotic manipulation inside scanning electron microscopes, Microsyst. Nanoeng. 2 (2016) 16024.
[7] G.M. Whitesides, B. Grzybowski, Self-assembly at all scales, Science 295 (2002) 2418–2421.
[8] Z.L. Wang, Triboelectric nanogenerators as new energy technology and self-powered sensors- principles, problems and perspectives, Faraday Discuss 176 (2015) 447–458.
[9] S.S. Kwak, H.J. Yoon, S.W. Kim, Textile-based triboelectric nanogenerators for self-powered wearable electronics, Adv. Funct. Mater. 29 (2019) 1804533.
[10] J. Kim, M. Lee, H.J. Shim, R. Ghaffari, H.R. Cho, D. Son, Y.H. Jung, M. Soh, C. Choi, S. Jung, K. Chu, D. Jeon, S.T. Lee, J.H. Kim, S.H. Choi, T. Hyeon, D.H. Kim, Stretchable silicon nanoribbon electronics for skin prosthesis, Nat. Commun. 5 (2013) 5747.
[11] Q. Shi, T. He, C. Lee, More than energy harvesting – Combining triboelectric nanogenerator and flexible electronics technology for enabling novel micro-/nano-

systems, Nano Energy 57 (2019) 851–871.
[12] Y. Hu, Z. Zheng, Progress in textile-based triboelectric nanogenerators for smart fabrics, Nano Energy 56 (2019) 16–24.
[13] W. Gao, S. Emaminejad, H.Y.Y. Nyein, S. Challa, K. Chen, A. Peck, H.M. Fahad, H. Ota, H. Shiraki, D. Kiriya, D.H. Lien, G.A. Brooks, R.W. Davis, A. Javey, Fully integrated wearable sensor arrays for multiplexed in situ perspiration analysis, Nature 529 (2016) 509–514.
[14] C. Wang, D. Hwang, Z. Yu, K. Takei, J. Park, T. Chen, B. Ma, A. Javey, User-interactive electronic skin for instantaneous pressure visualization, Nat. Mater. 12 (2013) 899–904.
[15] T. Chen, M. Zhao, Q. Shi, Z. Yang, H. Liu, L. Sun, J. Ouyang, C. Lee, Novel augmented reality interface using a self-powered triboelectric based virtual reality 3D-control sensor, Nano Energy 51 (2018) 162–172.
[16] M. Bariya, H.Y.Y. Nyein, A. Javey, Wearable sweat sensors, Nat. Electron. 1 (2018) 160–171.
[17] Q. Shi, H. Wu, H. Wang, H. Wu, C. Lee, Self-powered gyroscope ball using a triboelectric mechanism, Adv. Energy Mater. 7 (2017) 1701300.
[18] T. Chen, Y. Xia, W. Liu, H. Liu, L. Sun, C. Lee, A hybrid flapping-blade wind energy harvester based on vortex shedding effect, J. Microelectromech. S. 12 (2016) 845–847.
[19] H. Chen, Y. Song, X. Cheng, H. Zhang, Self-powered electronic skin based on the triboelectric generator, Nano Energy 56 (2019) 252–268.
[20] Q. Zheng, H. Zhang, B. Shi, X. Xue, Z. Liu, Y. Jin, Y. Ma, Y. Zou, X. Wang, Z. An, W. Tang, W. Zhang, F. Yang, Y. Liu, X. Lang, Z. Xu, Z. Li, Z.L. Wang, In vivo self-powered wireless cardiac monitoring via implantable triboelectric nanogenerator, ACS Nano 10 (2016) 6510–6518.
[21] Q. Shi, H. Wang, T. Wang, C. Lee, Self-powered liquid triboelectric microfluidic sensor for pressure sensing and finger motion monitoring applications, Nano Energy 30 (2016) 450–459.
[22] Y. Yang, H. Zhang, Z.H. Lin, Y.S. Zhou, Q. Jing, Y. Su, J. Yang, J. Chen, C. Hu, Z.L. Wang, Human skin based triboelectric nanogenerators for harvesting biomechanical energy and as self-powered active tactile sensor system, ACS Nano 7 (2013) 9213–9222.
[23] W. Yang, J. Chen, G. Zhu, J. Yang, P. Bai, Y. Su, Q. Jing, X. Cao, Z.L. Wang, Harvesting energy from the natural vibration of human walking, ACS Nano 7 (2013) 11317–11324.
[24] Y. Ma, Q. Zheng, Y. Liu, B. Shi, X. Xue, W. Ji, Z. Liu, Y. Jin, Y. Zou, Z. An, W. Zhang, X. Wang, W. Jiang, Z. Xu, Z.L. Wang, Z. Li, H. Zhang, Self-powered, one-stop, and multifunctional implantable triboelectric active sensor for real-time biomedical monitoring, Nano Lett. 16 (2016) 6042–6051.
[25] G.Q. Gu, C.B. Han, J.J. Tian, C.X. Lu, C. He, T. Jiang, Z. Li, Z.L. Wang, Antibacterial composite film-based triboelectric nanogenerator for harvesting walking energy, ACS Appl. Mater. Interfaces 9 (2017) 11882–11888.
[26] J. Zhu, X. Hou, X. Niu, X. Guo, J. Zhang, J. He, T. Guo, X. Chou, C. Xue, W. Zhang, The d-arched piezoelectric-triboelectric hybrid nanogenerator as a self-powered vibration sensor, Sensor. Actuat. A-Phys 263 (2017) 317–325.
[27] Z. Tian, J. He, X. Chen, Z. Zhang, T. Wen, C. Zhai, J. Han, J. Mu, X. Hou, X. Chou, C. Xue, Performance-boosted triboelectric textile for harvesting human motion energy, Nano Energy 39 (2017) 562–570.
[28] X. Liu, K. Zhao, Z.L. Wang, Y. Yang, Unity convoluted design of solid li-ion battery and triboelectric nanogenerator for self-powered wearable electronics, Adv. Energy Mater. 7 (2017) 1701629.
[29] G. Liu, J. Chen, Q. Tang, L. Feng, H. Yang, J. Li, Y. Xi, X. Wang, C. Hu, Wireless electric energy transmission through various isolated solid media based on triboelectric nanogenerator, Adv. Energy Mater. 8 (2018) 1703086.
[30] S.W. Chen, X. Cao, N. Wang, L. Ma, H.R. Zhu, M. Willander, Y. Jie, Z.L. Wang, An ultrathin flexible single-electrode triboelectric-nanogenerator for mechanical energy harvesting and instantaneous force sensing, Adv. Energy Mater. 7 (2017) 1601255.
[31] H. Wang, H. Wu, D. Hasan, T. He, Q. Shi, C. Lee, Self-powered dual-mode amenity sensor based on the water-air triboelectric nanogenerator, ACS Nano 11 (2017) 10337–10346.
[32] T. He, Q. Shi, H. Wang, F. Wen, T. Chen, J. Ouyang, C. Lee, Beyond energy harvesting - multi-functional triboelectric nanosensors on a textile, Nano Energy 57 (2019) 338–352.
[33] G. Liu, J. Chen, H. Guo, M. Lai, X. Pu, X. Wang, C. Hu, Triboelectric nanogenerator based on magnetically induced retractable spring steel tapes for efficient energy harvesting of large amplitude motion, Nano Res 11 (2018) 633–641.
[34] J. He, T. Wen, S. Qian, Z. Zhang, Z. Tian, J. Zhu, J. Mu, X. Hou, W. Geng, J. Cho, J. Han, X. Chou, C. Xue, Triboelectric-piezoelectric-electromagnetic hybrid nanogenerator for high efficient vibration energy harvesting and self-powered wireless monitoring system, Nano Energy 43 (2018) 326–339.
[35] R. Cao, X. Pu, X. Du, W. Yang, J. Wang, H. Guo, S. Zhao, Z. Yuan, C. Zhang, C. Li, Z.L. Wang, Screen-printed washable electronic textiles as self-powered touch/gesture tribo-sensors for intelligent human-machine interaction, ACS Nano 12 (2018) 5190–5196.
[36] Y. Yang, Y.S. Zhou, H. Zhang, Y. Liu, S. Lee, Z.L. Wang, A single-electrode based triboelectric nanogenerator as self-powered tracking system, Adv. Mater. 25 (2013) 6594–6601.
[37] H. Liu, Z. Ji, H. Xu, M. Sun, T. Chen, L. Sun, G. Chen, Z. Wang, Large-scale and flexible self-powered triboelectric tactile sensing array for sensitive robot skin, Polymers 9 (2017) 586.
[38] X. Pu, H. Guo, Q. Tang, J. Chen, L. Feng, G. Liu, X. Wang, Y. Xi, C. Hu, Z.L. Wang, Rotation sensing and gesture control of a robot joint via triboelectric quantization sensor, Nano Energy 54 (2018) 453–460.
[39] X. Chou, J. Zhu, S. Qian, X. Niu, J. Qian, X. Hou, J. Mu, W. Geng, J. Cho, J. He, C. Xue, All-in-one filler-elastomer-based high-performance stretchable piezoelectric nanogenerator for kinetic energy harvesting and self-powered motion monitoring, Nano Energy 53 (2018) 550–558.
[40] Y. Yang, H. Zhang, Z.H. Lin, Y.S. Zhou, Q. Jing, Y. Su, J. Yang, J. Chen, C. Hu, Z.L. Wang, Human skin based triboelectric nanogenerators for harvesting biomechanical energy and as self-powered active tactile sensor system, ACS Nano 7 (2013) 9213–9222.
[41] X. Cheng, L. Miao, Y. Song, Z. Su, H. Chen, X. Chen, J. Zhang, H. Zhang, High efficiency power management and charge boosting strategy for a triboelectric nanogenerator, Nano Energy 38 (2017) 438–446.
[42] Z. Yang, Q. Xu, X. Wang, J. Lu, H. Wang, F. Li, L. Zhang, G. Hu, C. Pan, Large and ultrastable all-inorganic CsPbBr3 monocrystalline films: low-temperature growth and application for high-performance photodetectors, Adv. Mater. (2018) 1802110.
[43] L. Jin, J. Tao, R. Bao, L. Sun, C. Pan, Self-powered real-time movement monitoring sensor using triboelectric nanogenerator technology, Sci. Rep. 7 (2017) 10521.
[44] J. Chen, X. Pu, H. Guo, Q. Tang, L. Feng, X. Wang, C. Hu, A self-powered 2D barcode recognition system based on sliding mode triboelectric nanogenerator for personal identification, Nano Energy 43 (2018) 253–258.
[45] H. Kim, J.H. Ahn, Graphene for flexible and wearable device applications, Carbon 120 (2017) 244–257.
[46] L. Cheng, Q. Xu, Y. Zheng, X. Jia, Y. Qin, A self-improving triboelectric nanogenerator with improved charge density and increased charge accumulation speed, Nat. Commun. 9 (2018) 3773.
[47] H. Liu, K.H. Koh, C. Lee, Ultra-wide frequency broadening mechanism for micro-scale electromagnetic energy harvester, Appl. Phys. Lett. 104 (2014) 053901.
[48] J. Cheng, W. Ding, Y. Zi, Y. Lu, L. Ji, F. Liu, C. Wu, Z.L. Wang, Triboelectric microplasma powered by mechanical stimuli, Nat. Commun. 9 (2018) 3733.
[49] Y. Zi, J. Wang, S. Wang, S. Li, Z. Wen, H. Guo, Z.L. Wang, Effective energy storage from a triboelectric nanogenerator, Nat. Commun. 7 (2016) 10987.
[50] S. Gong, W. Cheng, Toward soft skin-like wearable and implantable energy devices, Adv. Energy Mater. 7 (2017) 1700648.
[51] Z.L. Wang, G. Zhu, Y. Yang, S. Wang, C. Pan, Progress in nanogenerators for portable electronics, Mater. Today 15 (2012) 532–543.
[52] Z. Wen, M.H. Yeh, H. Guo, J. Wang, Y. Zi, W. Xu, J. Deng, L. Zhu, X. Wang, C. Hu, L. Zhu, X. Sun, Z.L. Wang, Self-powered textile for wearable electronics by hybridizing fiber-shaped nanogenerators, solar cells, and supercapacitors, Sci. Adv. 2 (2016) e1600097.
[53] P.K. Yang, Z.H. Lin, K.C. Pradel, L. Lin, X. Li, X. Wen, J.H. He, Z.L. Wang, Paper-based origami triboelectric nanogenerators and self-powered pressure sensors, ACS Nano 9 (2015) 901–907.
[54] P.K. Yang, L. Lin, F. Yi, X. Li, K.C. Pradel, Y. Zi, C.I. Wu, J.H. He, Y. Zhang, Z.L. Wang, A flexible, stretchable and shape-adaptive approach for versatile energy conversion and self-powered biomedical monitoring, Adv. Mater. 27 (2015) 3817–3824.
[55] S.F. Leung, K.T. Ho, P.K. Kung, V.K. Hsiao, H.N. Alshareef, Z.L. Wang, J.H. He, A self-powered and flexible organometallic halide perovskite photodetector with very high detectivity, Adv. Mater. 30 (2018) 1704611.
[56] J. Chun, N.R. Kang, J.Y. Kim, M.S. Noh, C.Y. Kang, D. Choi, S.W. Kim, Z.L. Wang, J.M. Baik, Highly anisotropic power generation in piezoelectric hemispheres composed stretchable composite film for self-powered motion sensor, Nano Energy 11 (2015) 1–10.
[57] J. Bian, N. Wang, J. Ma, Y. Jie, J. Zou, X. Cao, Stretchable 3D polymer for simultaneously mechanical energy harvesting and biomimetic force sensing, Nano Energy 47 (2018) 442–450.
[58] K.Y. Lee, M.K. Gupta, S.W. Kim, Transparent flexible stretchable piezoelectric and triboelectric nanogenerators for powering portable electronics, Nano Energy 14 (2015) 139–160.
[59] Y.C. Lai, J. Deng, S.L. Zhang, S. Niu, H. Guo, Z.L. Wang, Single-thread-based wearable and highly stretchable triboelectric nanogenerators and their applications in cloth-based self-powered human-interactive and biomedical sensing, Adv. Funct. Mater. 27 (2017) 1604462.
[60] B.U. Hwang, J.H. Lee, T.Q. Trung, E. Roh, D. Kim, S.W. Kim, N.E. Lee, Transparent stretchable self-powered patchable sensor platform with ultrasensitive recognition of human activities, ACS Nano 9 (2015) 8801–8810.
[61] G.H. Lim, S.S. Kwak, N. Kwon, T. Kim, H. Kim, S.M. Kim, S.W. Kim, B. Lim, Fully stretchable and highly durable triboelectric nanogenerators based on gold-nanosheet electrodes for self-powered human-motion detection, Nano Energy 42 (2017) 300–306.
[62] L. Yu, H. Song, T. Wang, Z. Wang, L. Sun, Z. Du, A new asymmetrical mass distribution method on the analysis of universal “force-sensing” model for 3-DOF translational parallel manipulator, Ind. Robot 41 (2014) 56–69.
[63] B. Hu, Y. Yao, P. Wu, Y. Lu, A Comparison Study of Two 3-UPU Translational Parallel Manipulators vol. 10, (2013), p. 190.
[64] O. Baser, I. Konukseven, 7-DOF haptic device and interface design, Turk. J. Electr. Eng. Co (2013) 493–499.
[65] J.B.H. Tok, Z. Bao, Recent advances in flexible and stretchable electronics, sensors and power sources, Sci. China Chem. 55 (2012) 718–725.
[66] M. Shi, J. Zhang, H. Chen, M. Han, S.A. Shankaregowda, Z. Su, B. Meng, X. Cheng, H. Zhang, Self-powered analogue smart skin, ACS Nano 10 (2016) 4083.
[67] T. Li, J. Zou, F. Xing, M. Zhang, X. Cao, N. Wang, Z.L. Wang, From dual-mode triboelectric nanogenerator to smart tactile sensor: a multiplexing design, ACS Nano 11 (2017) 3950–3956.
[68] H. Wu, Z. Su, M. Shi, L. Miao, Y. Song, H. Chen, M. Han, H. Zhang, Self-powered noncontact electronic skin for motion sensing, Adv. Funct. Mater. 28 (2018) 1704641.
[69] T. Chen, Q. Shi, M. Lu, T. He, L. Sun, L. Yang, C. Lee, Triboelectric self-powered

wearable flexible patch as 3D motion control interface for robotic manipulator, ACS Nano 12 (2018) 11561–11571.
[70] T. Chen, Q. Shi, K. Li, Z. Yang, H. Liu, L. Sun, J.A. Dziuban, C. Lee, Investigation of position sensing and energy harvesting of a flexible triboelectric touch pad, Nanomaterials 8 (2018) 613.

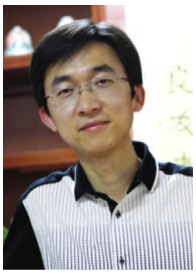

Tao Chen received the B.Sc. degree in Mechanical Design, Manufacturing and Automation, M.Sc. degree in Mechatronic Engineering, and Ph.D. degree in Mechatronic Engineering from Harbin Institute of Technology, Harbin, China, in 2004, 2006, and 2010, respectively. He is a visiting scholar in National University of Singapore in 2018. He is currently an associate professor at Soochow University, Suzhou, China. His main research interests include MEMS, sensors, and actuators.

Qiongfeng Shi received his B.Eng. degree from Department of Electronic Engineering and Information Science at University of Science and Technology of China (USTC) in 2012. He is currently pursuing his Ph.D. degree in the Department of Electrical and Computer Engineering, National University of Singapore (NUS) under the NUS research scholarship. His research interests are focused on energy harvesters and self-powered sensors.

Minglu Zhu Received his B.Bus. degree in Business Administration from the School of Business at State University of Bangladesh, Dhaka, Bangladesh, in 2010, and B.Sc. degree in Materials Science and Engineering from the School of Materials Science and Engineering at University of Illinois at Urbana-Champaign, Illinois, United States, in 2014. He is now a Ph.D. student at the Department of Electrical & Computer Engineering, NUS. His research interests focus mainly on MEMS based energy harvesters and self-powered sensors.

Tianyiyi He received her B.Eng. degree from the School of Microelectronics and Solid-state Electronics at the University of Electronic Science and Technology of China (UESTC), Chengdu, China, in 2016. She is now a Ph.D. candidate in the Department of Electrical and Computer Engineering, National University of Singapore. Her research interests include energy harvesters, triboelectric nanogenerator, thermoelectric energy harvester, and self-powered sensors.

Zhan Yang received B.S.in department of automation in Harbin University of Science and Technology, M.S. and Dr. Eng. in department of micronano system of Nagoya University in 2010 and 2013.He is Associate Professor in Robotics and Microsystem Center, Soochow University, Suzhou, China and Collaborative Innovation Center of Suzhou Nano Science and Technology, Soochow University. He is Secretary-General of China Society of Micro-Nano Robotics. His research interest in nano manipulation, nano sensor and nano robotics. He has published more than 30 papers on micronano manipulation and their applications.

Huicong Liu received her Ph.D. degree from the Department of Mechanical Engineering, National University of Singapore (NUS) in 2013. She has been a Research Fellow in Department of Electrical and Computer Engineering, NUS from Aug. 2012 to Aug. 2013. Currently she is an Associate Professor in Robotics and Microsystems Center, School of Mechanical & Electric Engineering, Soochow University, China. Her research interests are vibration-based MEMS/NEMS energy harvesters, self-powered MEMS/NEMS system for IoTs and flexible functional devices for robotic and medical applications.

Lining Sun is a currently a director of Robotics and Microsystems Center in Soochow University, and a President of College of Mechatronic Engineering in Soochow University. He gained China National Funds for Distinguished Young Scientists. His current research interests include micro-nano operational robot and equipment, advanced robot and control, and electromechanical integration equipment. He gained two National Science and Technology Award Grade II and three Provincial Science and Technology Prize Grade I. He has more than 300 academic papers being published and has more than 20 patents of invention being authorized.

Lei Yang received Ph.D. in Materials Science and M.S. in Innovation Management and Entrepreneurship from Brown University, USA, and both M.E. and B.E. in Materials Science and Engineering from Tsinghua University, PR China. He has published over 50 papers in high-profile journals and authored 2 books by Elsevier. His research has also generated 23 Chinese patent applications. He serves as the Associate Editor-in-Chief of International Journal of Nanomedicine and an Editor of the book series of Biomaterials. He is the senior member or member of Chinese Society for Biomaterials, Chinese Materials Research Society, and Chinese Mechanical Engineering Society.

Chengkuo Lee received his Ph.D. degree in Precision engineering from The University of Tokyo in 1996. Currently, he is the director of Center for Intelligent Sensors and MEMS, and an Associate Professor in the Department of Electrical and Computer Engineering, National University of Singapore, Singapore. In 2001, he cofounded Asia Pacific Microsystems, Inc., where he was the Vice President. From 2006 to 2009, he was a Senior Member of the Technical Staff at the Institute of Microelectronics, A-STAR, Singapore. He has contributed to more than 300 international conference papers and extended abstracts and 290 peer-reviewed international journal articles.